Ultraviolet Resonance Raman Spectroscopy of Distamycin Complexes with Poly(dA)–Poly(dT) and Poly(dA-dT): Role of H-Bonding†

Christine A. Grygon and Thomas G. Spiro*

Department of Chemistry, Princeton University, Princeton, New Jersey 08544-1009

Received December 5, 1988; Revised Manuscript Received February 8, 1989

ABSTRACT: Raman spectra are reported for distamycin, excited at 320 nm, in resonance with the first strong absorption band of the chromophore. Qualitative band assignments to pyrrole ring and amide modes are made on the basis of frequency shifts observed in D_2O. When distamycin is dissolved in dimethyl sulfoxide or dimethylformamide, large (30 cm^{-1}) upshifts are seen for the band assigned to amide I, while amides II and III shift down appreciably. Similar but smaller shifts are seen when distamycin is bound to poly(dA-dT) and poly(dA)–poly(dT). Examination of literature data for *N*-methylacetamide in various solvents shows that the amide I frequencies correlate well with solvent acceptor number but poorly with solvent donor number. This behavior implies that acceptor interactions with the C=O group are more important than donor interactions with the N–H group in polarizing the amide bond and stabilizing the zwitterionic resonance form. The resonance Raman spectra therefore imply that the distamycin C=O groups, despite being exposed to solvent, are less strongly H-bonded in the polynucleotide complexes than in aqueous distamycin, perhaps because of orienting influences of the nearby backbone phosphate groups. In this respect, the poly(dA-dT) and poly(dA)–poly(dT) complexes are the same, showing the same RR frequencies. Resonance Raman spectra were also obtained at 200-nm excitation, where modes of the DNA residues are enhanced. The spectra were essentially the same with and without distamycin, except for a perceptable narrowing of the adenine modes of poly(dA-dT), suggesting a reduction in conformational flexibility of the polymer upon drug binding.

Distamycin and netropsin are natural toxins whose molecular structures (see Figure 1) contain pyrrole rings connected by peptide bonds. They bind strongly to double-helical DNA strands containing A-T base pairs but only weakly to G-C tracts (Zimmer et al., 1971; Wartell et al., 1974; Zimmer, 1975; Krey et al., 1973; Zasedatelov et al., 1974; Patel & Canuel, 1977). Crystal structures have been reported for B-form DNA dodecamers with bound netropsin (Kopka et al., 1985) and distamycin (Coll et al., 1987), and previous NMR results indicate the same netropsin–dodecamer geometry in solution (Patel, 1982). In each case the drug molecule fits into the minor groove of the double helix with its peptide NH protons involved in bifurcated H-bonds to N3 atoms of adenine and C2=O atoms of thymine residues. In addition the amidinium groups at the ends of both molecules and the guanidinium group at the other end of netropsin form H-bonds to adenine N3 atoms and are involved in nonspecific electrostatic interactions with the negatively charged phosphate groups of the DNA backbone. The remaining interactions are van der Waals in character, there being a close fit between the curved ribbon drug molecules and the walls of the minor groove. Similar binding to G-C stretches is prevented by the steric hindrance of the C6–NH_2 substituents on the G residues. The thermodynamics of netropsin binding have been studied by Marky and Breslauer (Marky et al., 1983, 1984; Marky & Breslauer, 1987).

While X-ray crystallography has defined the structure of the drug–DNA complex, it is not clear to what extent the various intermolecular contacts contribute to the binding energy. Theoretical calculations have been carried out by Pullman and co-workers (Zakrzewska et al., 1983; Zakrzewska & Pullman, 1983) and by Caldwell and Kollman (1986), who obtained general consistency with the experimental data on the mode of netropsin binding, but important details were rendered uncertain by the difficulty of including solvation and electrostatics in the potential. Vibrational spectroscopy can provide useful insights since molecular vibrations are perturbed to the extent that intermolecular interactions are strong. In the present study we examine the Raman spectrum of distamycin free in solution and bound to poly(dA-dT) and to poly(dA)–poly(dT), using the resonance enhancement provided by the near-ultraviolet electronic transition of the drug to label its vibrational modes. Martin et al. (1978) have previously recorded the Raman spectrum of distamycin and of its complex with calf thymus DNA using visible excitation. Their data are consistent with ours, but the vibrational bands were misassigned, obscuring the structural interpretation. We find that frequencies associated with the distamycin amide bonds show shifts upon polynucleotide binding that imply *weaker* H-bonding in the complex than in aqueous solution. On the basis of the solvent dependence of amide frequencies, we conclude that this effect probably results from limited access by H_2O molecules to the distamycin carbonyl groups when the drug lies in the DNA minor groove.

Raman bands of the nucleic acid bases have also been examined via 200-nm excitation in resonance with strong electronic transitions of A and T. Distamycin binding does not shift any of the base mode frequencies, but the bands narrow noticeably for the poly(dA-dT) complex. This observation suggests that distamycin reduces the conformational mobility of the residues in the polymer.

Experimental Procedures

Distamycin hydrochloride was purchased from Sigma and used without further purification. Spectral-grade DMSO and

† This work was supported by NIH Grant GM25158.

* Author to whom correspondence should be addressed.

0006-2960/89/0428-4397$01.50/0

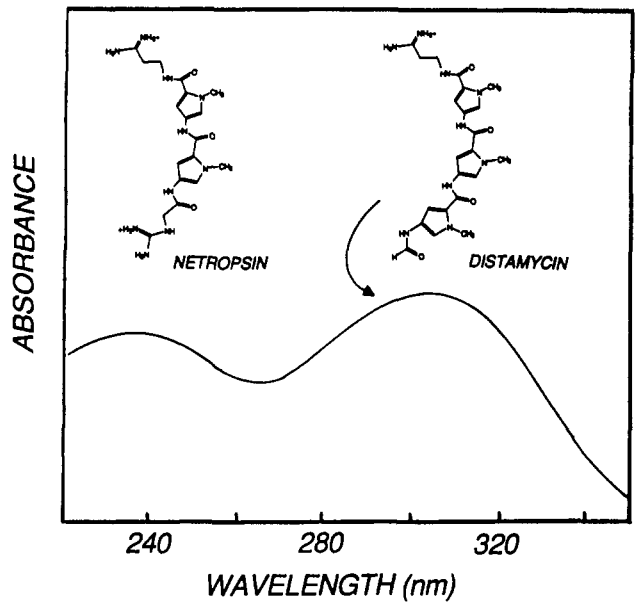

FIGURE 1: Ultraviolet absorption spectrum of aqueous distamycin. Also shown are the molecular structures of distamycin and netropsin.

DMF were obtained from Baker. Distamycin samples for Raman spectroscopy were prepared at a concentration of 10–20 absorbance units/mL at 300 nm [H_2O and D_2O solutions also contained 50 mM phosphate buffer at pH (or pD) 7]. The polynucleotides were obtained from Pharmacia Molecular Biologicals as lyophilized sodium salts and were dissolved in 50 mM phosphate buffer (pH 7) at a concentration of 20 OD units/mL at 260 nm. Drug binding was induced via the dropwise addition of a concentrated distamycin solution to the polynucleotide to give a 10:1 or 6:1 (base pair:drug) molar ratio. Concentrations were determined spectrophotometrically [ϵ_{300} (distamycin) = 37 000 M^{-1} cm^{-1} (Arcamone et al., 1967); ϵ_{260} (poly(dA)–poly(dT)) = 6000 M^{-1} cm^{-1} (Chamberlin, 1965); ϵ_{260} (poly(dA-dT)) = 6700 M^{-1} cm^{-1} (Radding & Kornberg)], and binding was confirmed via the bathochromic shift of the long-wavelength distamycin absorption band to 320 nm. The complexes were allowed to equilibrate overnight at 4 °C. Absorption spectra were measured with a Hewlett-Packard 8451A diode array spectrophotometer.

Instrumentation for obtaining ultraviolet resonance Raman spectra has been described previously (Fodor et al., 1986) and employs the output of the second and fourth harmonics of a Q-switched Nd:YAG pulsed laser. A recirculating open flow cell was used for the aqueous samples. For the measurements in organic solvents, the samples were enclosed in 1-cm high-quality quartz cuvettes and magnetically stirred.

Results and Discussion

Figure 2 shows RR spectra for distamycin dissolved in H_2O, D_2O, dimethyl sulfoxide (DMSO), and dimethylformamide (DMF), obtained with 320-nm (or 299-nm) excitation. These wavelengths lie within the first strong electronic absorption band, shown in Figure 1. The electronic transition which gives rise to this band is no doubt delocalized over the conjugated pyrrole–amide system. Both amide and pyrrole ring vibrational modes are therefore expected to be enhanced. The amide bonds should give rise to three modes in the region between 1000 and 1700 cm^{-1}, amides I, II, and III (Frushour & Koenig, 1975; Williams, 1983; Mayne et al., 1985). Amide I, which is generally found near 1650 cm^{-1}, is a C=O stretching mode primarily, while amides II and III, found near 1550 and 1250 cm^{-1}, are mixtures of C–N stretching and N–H bending co-

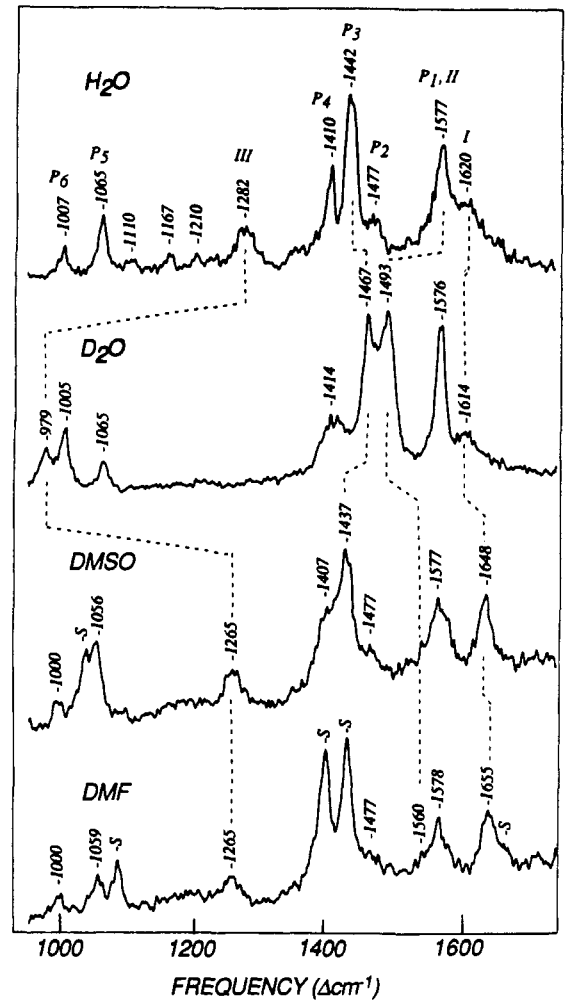

FIGURE 2: UV resonance Raman spectra for distamycin dissolved in various solvents. Aqueous spectra were obtained with 320-nm excitation, while spectra in DMSO and DMF were obtained with 299-nm excitation. Amide modes I, II, and III are marked in the H_2O spectrum. Dotted lines indicate correlations of these frequencies in the other solvents. Bands marked with an S are due to solvent.

ordinates (Frushour & Koenig, 1975; Williams, 1983; Mayne et al., 1985). When the N–H proton is replaced by deuterium, these coordinates are unmixed, leaving a nearly pure C–N stretch at 1450 cm^{-1} (amide II′) and N–D bend at 950 cm^{-1} (amide III′). We therefore assign amide I, II, and III in aqueous distamycin to bands at 1620, 1577, and 1282 cm^{-1}, on the basis of their shifts in D_2O to 1614, 1493, and 979 cm^{-1}, as shown in Figure 2.

The 1577-cm^{-1} band is a composite of amide II and another mode, revealed as a sharpened band at 1576 cm^{-1} in the D_2O solution. Five pyrrole ring modes are expected, which involve stretching of the five ring bonds with different relative phasing. These are tentatively identified with the relatively strong RR bands at 1577, 1477, 1442, 1410, and 1065 cm^{-1} and labeled P_1–P_5. These frequencies are compared with those of the ring modes of pyrrole itself in Table I, where it can be seen that there is a reasonable correspondence even though appreciable mixing of the pyrrole and amide modes is expected. Direct evidence for such mixing is the substantial upshift, 1442 to 1467 cm^{-1}, for one of the ring modes when distamycin is dissolved in D_2O.

Pyrrole also has four C–H bending modes in the frequency region under consideration, but only two are expected for distamycin since substitution on the ring reduces the number of ring protons to two. We tentatively assign these to weak bands at 1210 and 1167 cm^{-1}. Two other bands, 1110 and

Table I: Distamycin UVRR Frequency (cm^{-1}) Correlations and Tentative Assignments

	medium					
mode	H_2O	D_2O	DMSO	DMF	poly(dA-dT)	pyrrole[a]
amide I	1620	1614	1648	1655	1632	
amide II	1577	1493		1560	1560	
Pyr ring (P_1)	1577	1576	1577	1578	1579	1530
Pyr ring (P_2)	1477	*b*	1474	1474	1477	1467
Pyr ring (P_3)	1442	1467	1437	*d*	1435	1418
Pyr ring (P_4)	1410	1414	1407	*d*	1410	1379
amide III	1282	979	1265	*d*	1274	
Pry δCH	1210	*c*	*c*	*c*	1199	1237
Pyr δCH	1167	*c*	*c*	*c*	1164	1076
Pyr C	1110	*c*	*c*	*c*	1108	
Pyr ring (P_5)	1065	1065	1056	1059	1064	1144
Pyr N (P_6)	1007	1005	1000	1000	1003	1015

[a] Frequencies of the pyrrole molecule; assignments from Dollish et al. (1974). [b] Position obscured by nearby strong bands. [c] Too weak for observation. [d] Obscured by solvent bands.

1007 cm^{-1}, are probably associated with stretching of the N–C and C–C single bonds in the amide linkage between the pyrrole rings.

These assignments tacitly assume that the mode frequencies are the same for the three pyrrole rings and four amide groups in distamycin. No doubt the couplings among these spatially separate units are small, but they may account for some of the bands being rather broad.

The 488-nm-excited Raman spectrum of aqueous distamycin, reported a decade ago by Martin et al. (1978), is quite similar in band frequencies and relative intensities to the 320-nm-excited RR spectrum. We infer that the 488-nm intensities are determined by preresonance enhancement from the 320-nm electronic transition. To make assignments, Martin et al. (1978) carried out a normal coordinate analysis and matched observed and calculated frequencies. Unfortunately, this procedure is unreliable in the absence of isotopic frequency shifts to identify the modes, since the calculation cannot be expected to be accurate enough to distinguish among alternative correspondences among the numerous observed and calculated frequencies. As a result, Martin et al. misassigned key bands, including the 1620-cm^{-1} amide I band, assigned instead to a ring mode, and the 1442-cm^{-1} band, assigned to a methyl group deformation mode. (Methyl deformations do not generally give rise to strong Raman bands, and the large D_2O shift clearly precludes this assignment.) Because of these misassignments, their Raman spectrum of distamycin bound to DNA, which showed features similar to our RR spectra (see next section), could not be properly interpreted.

Frequency Shifts and H-Bonding. When the distamycin RR spectrum in H_2O is compared to those in DMSO and DMF (Figure 2), the pyrrole ring modes are found at nearly the same frequencies, but there are significant shifts in the amide bands. Amide I shifts up by 28 cm^{-1} (DMSO) and 35 cm^{-1} (DMF), while amide III shifts down by 17 cm^{-1}. A 17-cm^{-1} downshift is also suggested for amide II by the shoulder at 1560 cm^{-1} seen on the 1577-cm^{-1} ring mode in DMSO and DMF. The 1442-cm^{-1} pyrrole ring mode, which is coupled to the amide modes, shifts down slightly, by 5 cm^{-1} in DMSO. (It is obscured by solvent bands in DMF.) These shifts are attributed to the changes in H-bonding of the amide groups, which have appreciable C=N double bond character (Schulz & Schirmer, 1979), resulting from a significant contribution of the zwitterionic resonance form shown in Figure 3. This form is stabilized by H-bond donation to the carbonyl O atom or H-bond acceptance from the N–H protons. The result is a weakening of the C=O bond and a strengthening of the C–N bond producing a downshift in amide I and upshifts in amides II and III. Water molecules can act as both H-bond donors and acceptors while DMSO and DMF are only acceptors. Thus stabilization of the zwitterionic resonance structure is greater for water, and the amide frequencies are shifted accordingly.

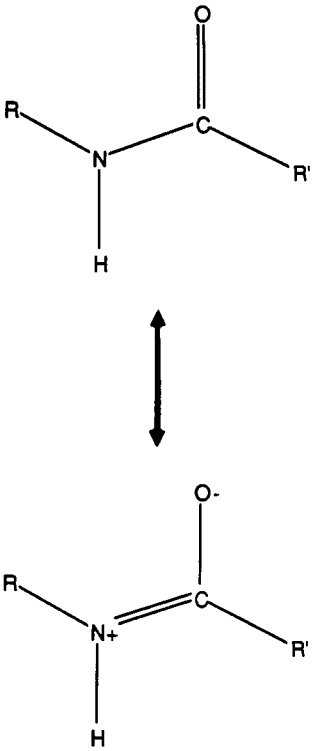

FIGURE 3: Resonance structures for the amide bond: neutral and zwitterionic forms.

RR spectra of distamycin bound to poly(dA-dT) and to poly(dA)–poly(dT) are shown in Figure 4. Downshifts are clearly seen, relative to the aqueous distamycin spectrum, in the frequencies of amides II and III and the 1442-cm^{-1} ring mode, and an upshift is seen for amide I. This pattern is similar to that of distamycin in DMSO and DMF. The amide II and ring mode shifts are as large as those seen in DMSO while the amide I and III shifts are about half as large. The lack of exact parallelism probably means that factors other than H-bonding, e.g., conformational changes between distamycin free in solution and bound to the polymers, play a role in determining the vibrational frequencies. Nevertheless it is clear that stabilization of the zwitterionic amide resonance form is somewhat greater for the DNA complexes than for distamycin in DMSO but is appreciably less than for aqueous distamycin. This result seems paradoxical, since the H-bonds from the distamycin NH protons to the A and T acceptor atoms, which are clearly established by crystallography (Coll et al., 1987), might have been expected to stabilize the zwitterionic form more than water.

In order to understand this phenomenon we have examined data in the literature on the amide I frequency of *N*-methylacetamide in various solvents (Cutmore & Hallam, 1969). In Figure 5, we plot these frequencies against donor number and/or acceptor number of the solvent (Gutman, 1976). The donor number is a measure of solvent nucleophilicity, measured as the enthalpy of adduct formation with a strong Lewis base, $SbCl_5$; solvents with larger donor numbers should be stronger acceptors of H-bonds from the amide N–H protons. Conversely, solvents with larger acceptor numbers should interact more strongly with the negatively charged

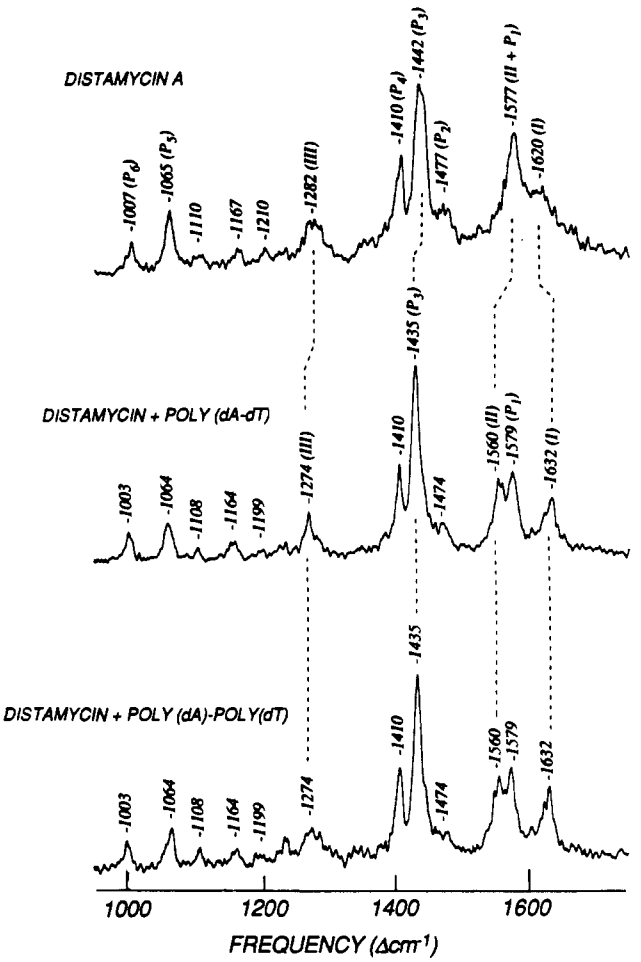

FIGURE 4: UV resonance Raman spectra, with 320-nm excitation, for free distamycin and distamycin bound to the A-T polynucleotides. Molar drug to base pair ratio employed in the complexes was 1:10 to minimize the concentration of free drug in solution. Pyrrole ring and amide modes are numbered and labeled as in Table I. Spectra are the average of 5–10 single scans.

carbonyl O atom, the acceptor number being determined by the tendency for adduct formation with the donor $(C_2H_5)_3$-P=O. It can be seen that the *N*-methylacetamide frequencies correlate well with the acceptor number but not at all with the donor number of the solvent. Linear correlations of C=O stretching frequencies with solvent acceptor numbers have been demonstrated for a number of carbonyl compounds, including *N*,*N*-diethylacetamide and dimethylformamide (Wohar et al.). These two compounds have quite different slopes, −1.56 and −0.99, respectively, consistent with a greater polarizability of the C=O bond in *N*,*N*-diethylacetamide due to the extra methyl groups. The slope for *N*-methylacetamide (Figure 5) is −0.97, essentially the same as for dimethylformamide. These two compounds, which are isomers, therefore show the same C=O bond polarizability even though N–H hydrogen bonding is precluded for dimethylformamide. The behavior of *N*-methylacetamide implies that interactions with the carbonyl group are the major determinants of the amide I frequency, while N–H interactions have little influence.

At first sight this result is surprising since both donor and acceptor interactions would be expected to stabilize the zwitterionic resonance form. However, the developing negative charge is concentrated on the carbonyl O atom, which is exposed directly to the solvent, while the positive charge on the N atom is delocalized over the three attached atoms. We note that the partial charges estimated for crystalline amides, which are extensively H-bonded, are −0.38 for the O atom but only

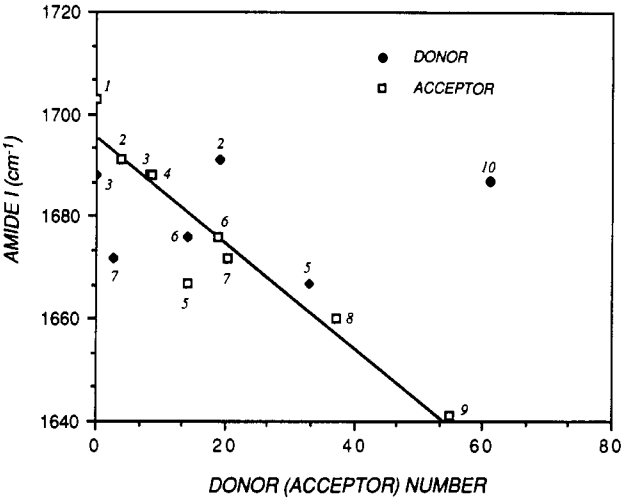

FIGURE 5: Plot of amide I frequency for *N*-methylacetamide vs donor (◆) and acceptor (□) number (Gutman, 1976). There is a good correlation for acceptor number (straight line) but none for donor number. The numerals refer to the following solvents: (1) *n*-hexane, (2) di-*n*-butyl ether, (3) benzene, (4) carbon tetrachloride, (5) pyridine, (6) acetonitrile, (7) nitromethane, (8) ethanol, (9) water, and (10) triethylamine. Amide I frequencies were obtained from IR data of Cutmore and Hallam (1969), except for the H_2O value, which was obtained from Raman data of Dudik et al. (1985).

+0.28 for the NH H atom (Hagler et al., 1984). Moreover, the O atom can accept two H-bonds, via its lone pairs, while the NH proton can only donate one H-bond (Rossky & Karplus, 1979).

While further investigation of this interesting phenomenon is clearly needed, the correlation in Figure 5 suggests that the amide I frequency mainly reflects carbonyl interactions. Whether this is also true for the amide II and III frequencies cannot be determined from the available data, but all three amide frequencies should be correlated if stabilization of the zwitterionic resonance form is the major variable. There may of course be other sources of variation, especially conformational effects which alter the normal mode compositions. For example, the differential in the amide mode shifts relative to that in aqueous solution for distamycin in DMSO and bound to DNA may result from the slight alteration of the interplanar angles of the pyrrole rings seen in the dodecamer complex (Coll et al., 1987), which might change the amide–pyrrole mixing somewhat.

In extending the inferences drawn from the *N*-methylacetamide data to distamycin, we note that the amide I frequencies in water, 1640 and 1620 cm^{-1}, respectively, differ substantially. The lower frequency for distamycin reflects the effect of conjugation with the pyrrole rings. However, the increase in the distamycin amide I frequency in DMSO, 28 cm^{-1}, is close to the increase, 35 cm^{-1}, expected from the slope of the line in Figure 5 (DMSO acceptor number = 19.3). Thus the polarization of the amide bond by acceptor solvents appears not to differ appreciably between distamycin and *N*-methylacetamide. We conclude that the amide I frequency in distamycin, like *N*-methylacetamide, is probably not very sensitive to the extent of NH H-bonding but is determined mainly by interactions of the carbonyl groups. The observed frequency in the DNA complexes represents an environment halfway between water and DMSO in its acceptor properties. The crystal structure (Coll et al., 1987) shows the distamycin carbonyls to be pointing out from the minor groove and accessible to solvent. Nevertheless, the RR data imply that interactions with solvent molecules are significantly weaker than those in aqueous solution. The structural basis for this weakening is not obvious. One possibility is that the water

molecules are ordered by the nearby charged phosphate groups of the DNA backbone in orientations that are unfavorable for interaction with the distamycin C=O groups.

Regardless of the origin of the amide I upshift, the implied destabilization of the zwitterionic resonance form relative to aqueous distamycin means a *negative* contribution to the binding energy. This negative contribution is overcome by positive contributions from electrostatic forces, H-bonding, and hydrophobic interactions. Breslauer et al. (1987) determined the thermodynamics of netropsin binding to DNA and have made the interesting observation that the binding is enthalpy driven in poly(dA-dT) but entropy driven in poly(dA)–poly(dT), even though the overall free energy is nearly the same. Dickerson et al. (1985) suggested that this difference might result from a more extensive hydration spine for the homopolymer duplex, whose displacement by the drug would release more entropy and also produce less enthalpy. On the other hand, Caldwell and Kollman (1986) suggested that there may be intrinsic differences in the H-bond pattern for netropsin binding to the two duplexes on the basis of different calculated structures, although they pointed out the uncertainty in their calculation occasioned by the lack of solvent or counterions. The available crystal structures offer no guidance on this question since the DNA dodecamers employed in the crystallizations contained AATT and AAATTT sequences, with regions of both alternating and nonalternating base pairs. The RR spectra are essentially the same for distamycin bound to poly(dA-dT) and poly(dA)–poly(dT) and offer no support for different structures, although the spectra may not be sensitive to alternative H-bonding modes of the N–H groups, for the reasons discussed above. The fact that the amide I frequency shows no difference implies that the water structure near the bound distamycin is the same for the two complexes.

DNA Effects. RR spectra with 200-nm excitation are shown in Figure 6 for the two duplexes with and without bound distamycin. At this wavelength ring modes of the bases are strongly enhanced (Grygon & Spiro, 1989; Tsuboi et al., 1987), and exocyclic modes (C=O stretching, NH_2 scissors) can also be detected in the 1600–1700-cm^{-1} region. These modes are identified in the figure.

The loading of the distamycin in the complexes was 6:1 (base pair:drug molecule), so that 85% of the base pairs should be involved in H-bonds from the distamycin NH groups (Coll et al., 1987). No frequency shifts are seen for any of the DNA bands, nor are there significant intensity changes upon drug binding. Thus the H-bonds are without detectable influence on the Raman bands. The significance of this result is uncertain because there are no models for the interactions seen in the crystal structures. We have no basis for anticipating the effect of H-bonding to N3 of adenine, although H-bonding at N7 appears to have a large intensity effect on selected adenine bands (Grygon et al., 1989). The H-bonds to the C2=O groups of thymine cannot be probed with the currently accessible UV excitation wavelengths since the C2=O stretching band is too weak to be detected in these polynucleotides. This mode may be more enhanced with shorter wavelength excitation.

The one noticeable effect of drug binding on the DNA UVRR spectra is a narrowing of the bands in poly(dA-dT). This is especially apparent in the clear separation of the 1302/1338-cm^{-1} and 1483/1510-cm^{-1} bands in the distamycin complex, which are associated with adenine ring modes (Fodor et al., 1985; Fodor & Spiro, 1986; Grygon & Spiro, 1989). The poly(dA)–poly(dT) spectra were too noisy to determine whether a similar narrowing occurred. The broader bands seen

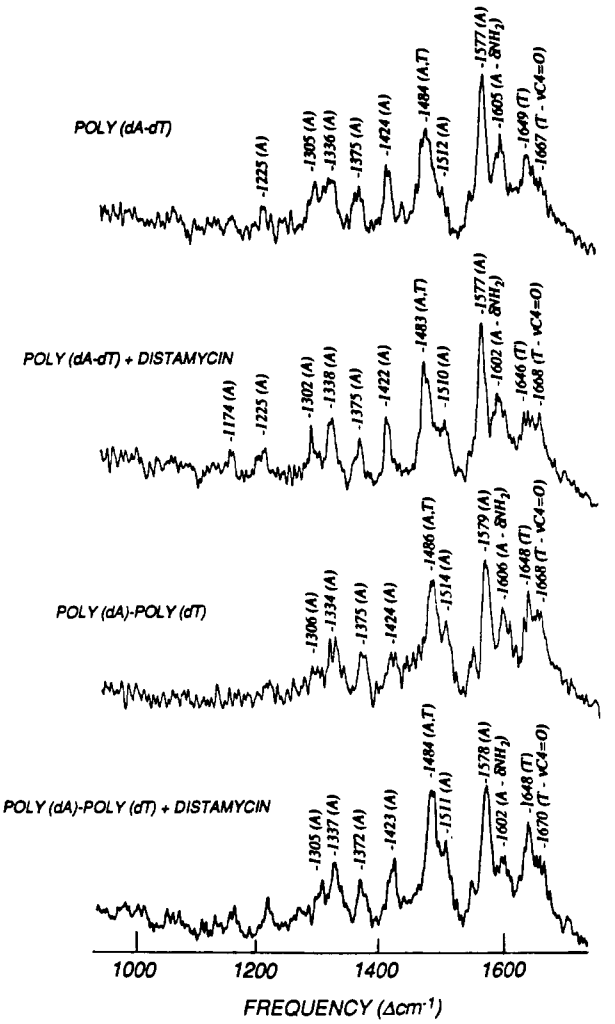

FIGURE 6: UV resonance Raman spectra, with 200-nm excitation, for poly(dA-dT) and poly(dA)–poly(dT) with and without bound distamycin. Molar drug to base pair ratio employed in the complexes was 1:6 to maximally load available binding sites on the nucleic acid. Major purine and pyrimidine ring mode contributors to the Raman peaks are noted with the appropriate letter (A or T). Band assignments for the exocyclic modes in the 1600–1700-cm^{-1} region are also indicated.

for poly(dA-dT) in the absence of distamycin probably result from somewhat different conformations of the DNA residues along the strand at any instant, producing a distribution of vibrational frequencies. The narrowing observed upon drug binding is therefore interpreted as reflecting restriction of the residue mobilities by the steric and H-bond interactions with the distamycin in the minor groove. This restriction produces more uniform residue conformations and narrower frequency distributions of the RR bands.

Conclusions

Excitation at 320-nm produces resonance-enhanced Raman spectra of distamycin showing strong bands associated with the amide and (coupled) pyrrole ring modes. The amide frequencies shift upon binding to poly(dA-dT) and poly(dA)–poly(dT) in a manner indicating weaker interactions of water molecules with the distamycin C=O groups, perhaps reflecting the ordering effects of the backbone phosphate groups. The available data suggest that the amide frequencies are insensitive to the degree of NH H-bonding and are therefore uninformative about the extent of distamycin NH interactions with the DNA bases, although the absence of any intensity effects on the 200-nm-excited UVRR spectra suggests

the absence of strong interactions. The DNA Raman bands sharpen noticeably upon distamycin binding, probably due to restricted conformational mobility of the bases.

References

Arcamone, F., Penco, S., Nicolella, V., Orezzi, P., & Pirelli, A. (1967) *Nature 203*, 1064.

Caldwell, J., & Kollman, P. (1986) *Biopolymers 25*, 249.

Chamberlin, M. J. (1965) *Fed. Proc., Fed. Am. Soc. Exp. Biol. 24*, 144.

Coll, M., Frederick, C. A., Wang, A. H.-J., & Rich, A. (1987) *Proc. Natl. Acad. Sci. U.S.A. 84*, 8385.

Cutmore, E. A., & Hallam, H. E. (1969) *Spectrochim. Acta 25A*, 1767.

Dollish, F. R., Fateley, W. G., & Bentley, F. F. (1974) in *Characteristic Raman Frequencies of Organic Compounds*, p 220, Wiley, New York.

Dudik, J. M., Johnson, C. R., & Asher, S. A. (1985) *J. Phys. Chem. 89*, 3805.

Fodor, S. P. A., & Spiro, T. G. (1986) *J. Am. Chem. Soc. 108*, 3198.

Fodor, S. P. A., Rava, R. P., Hays, T. R., & Spiro, T. G. (1985) *J. Am. Chem. Soc. 107*, 1520.

Fodor, S. P. A., Rava, R. P., Copeland, R. A., & Spiro, T. G. (1986) *J. Raman Spectrosc. 17*, 471.

Frushour, B. G., & Koenig, J. L. (1975) in *Advances in Infrared and Raman Spectroscopy* (Clark, R. J. H., & Hester, R. E., Eds.) Vol. 1, p 35, Heyden, New York.

Grygon, C. A., & Spiro, T. G. (1989) (submitted for publication).

Grygon, C. A., Davis, D. F., Spiro, T. G., & Fresco, J. R. (1989) *Proc. Natl. Acad. Sci. U.S.A.* (in press).

Gutman, V. (1976) *Coord. Chem. Rev. 18*, 225.

Hagler, A. T., Huler, E., & Lifson, S. (1984) *J. Am. Chem. Soc. 96*, 5319.

Kopka, M. L., Yoon, C., Goodsell, D., Pjura, P., & Dickerson, R. E. (1985) *Proc. Natl. Acad. Sci. U.S.A. 82*, 1376.

Krey, A. K., Allison, R. G., & Hahn, F. E. (1973) *FEBS Lett. 29*, 58.

Marky, L. A., & Breslauer, K. J. (1987) *Proc. Natl. Acad. Sci. U.S.A. 84*, 4359.

Marky, L. A., Blumenfeld, K. S., & Breslauer, K. J. (1983) *Nucleic Acids Res. 11*, 2857.

Marky, L. A., Currey, J., & Breslauer, K. J. (1984) in *The Molecular Basis of Cancer* (Rein, R., Ed.) Liss, New York.

Martin, J. C., Wartell, R. M., & O'Shea, D. (1978) *Proc. Natl. Acad. Sci. U.S.A. 11*, 5483.

Mayne, L. C., Ziegler, L. D., & Hudson, B. (1985) *J. Phys. Chem. 89*, 3395.

Patel, D. J. (1982) *Proc. Natl. Acad. Sci. U.S.A. 79*, 6424.

Patel, D. J., & Canuel, L. L. (1977) *Proc. Natl. Acad. Sci. U.S.A. 74*, 5207.

Radding, C. M., & Kornberg, A. (1962) *J. Biol. Chem. 237*, 2877.

Rossky, P. J., & Karplus, M. (1979) *J. Am. Chem. Soc. 101*, 1913.

Schulz, G. E., & Schirmer, A. H. (1979) in *Principles of Protein Structure* (Cantor, C. R., Ed.) p 18, Springer-Verlag, New York.

Tsuboi, M., Nishimura, Y., Hirakawa, A. Y., & Peticolas, W. L. (1987) in *Biological Applications of Raman Spectroscopy* (Spiro, T. G., Ed.) Vol. 2, p 109, Wiley, New York.

Wartell, R. M., Larson, J. E., & Wells, R. D. (1974) *J. Biol. Chem. 249*, 6719.

Williams, R. W. (1983) *J. Mol. Biol. 166*, 581.

Wohar, M. W., Seehra, J. K., & Jagodzinski, P. W. (1988) *Spectrochim. Acta 44A(10)*, 1006.

Zakrzewska, K., & Pullman, B. (1983) *Nucleic Acids Res. 11*, 8841.

Zakrzewska, K., Lavery, R., & Pullman, B. (1983) *Nucleic Acids Res. 11*, 8825.

Zasedatelov, A. S., Gursky, G. V., Zimmer, Ch., & Thrum, H. (1974) *Mol. Biol. Rep. 1*, 337.

Zimmer, Ch. (1975) in *Progress in Nucleic Acid Research and Molecular Biology* (Cohn, W. E., Ed.) p 285, Academic, New York.

Zimmer, Ch., Reinert, K. E., Luck, G., Wahnert, U., Lober, G., & Thrum, H. (1971) *J. Mol. Biol. 58*, 329.